Energy Metabolism in the Rat Cortex Under Thiopental Anaesthesia Measured *In Vivo* by ^{13}C MRS

Sarah Sonnay,[1] **João M. N. Duarte,**[1]★ **Nathalie Just,**[2]† **and Rolf Gruetter**[1,3,4]

[1]Laboratory for Functional and Metabolic Imaging, École Polytechnique Fédérale Lausanne, Switzerland
[2]Centre d'Imagerie Biomédicale – Animal and Technology Core, Lausanne, Switzerland
[3]Department of Radiology, University of Geneva, Switzerland
[4]Department of Radiology, University of Lausanne, Switzerland

Barbiturates, commonly used as general anaesthetics, depress neuronal activity and thus cerebral metabolism. Moreover, they are likely to disrupt the metabolic support of astrocytes to neurons, as well as the uptake of nutrients from circulation. By employing ^{13}C magnetic resonance spectroscopy (MRS) *in vivo* at high magnetic field, we characterized neuronal and astrocytic pathways of energy metabolism in the rat cortex under thiopental anaesthesia. The neuronal tricarboxylic acid (TCA) cycle rate was $0.46 \pm 0.02 \, \mu$mol/g/min, and the rate of the glutamate-glutamine cycle was $0.09 \pm 0.02 \, \mu$mol/g/min. In astrocytes, the TCA cycle rate was $0.16 \pm 0.02 \, \mu$mol/g/min, accounting for a quarter of whole brain glucose oxidation, pyruvate carboxylase rate was $0.02 \pm 0.01 \, \mu$mol/g/min, and glutamine synthetase was $0.12 \pm 0.01 \, \mu$mol/g/min. Relative to previous experiments under light α-chloralose anaesthesia, thiopental reduced oxidative metabolism in neurons and even more so in astrocytes. Interestingly, total oxidative metabolism in the cortex under thiopental anaesthesia surpassed the rate of pyruvate production by glycolysis, indicating substantial utilisation of substrates other than glucose, likely plasma lactate. © 2017 Wiley Periodicals, Inc.

Key words: glucose; metabolism; MRS; thiopental; α-chloralose; neuron-glia interaction

INTRODUCTION

Brain function is supported by sustained supply of oxygen and nutrients from the blood stream and relies on synchronized metabolic interaction between neurons and astrocytes (Hertz et al., 2007; Hyder and Rothman, 2012; Lanz et al., 2013). Anaesthetics modulate basal neuronal activity, and modify the coupling between neuronal activity and vascular regulation of blood flow and volume, which has been suggested to involve astrocytic signalling (Masamoto et al., 2012).

Barbiturates are widely used as anaesthetics or anti-convulsant agents by acting on the GABA$_A$ receptor thereby increasing the opening duration of the Cl$^-$ channel, leading to hyperpolarisation of the plasma membrane of target cells (Ito et al., 1996). At elevated dose, barbiturates can be used to profoundly depress cerebral activity and concomitantly reduce glucose metabolism (Hodes et al., 1985; Nilsson and Siesjo, 1975; Sokoloff et al., 1977; Strang and Bachelard, 1973; Crane et al., 1978). Additionally, barbiturates can directly depress mitochondrial respiration (e.g., Aldridge and Parker, 1960; Chance and Hollunger, 1963), further contributing to their role in depressing brain energy metabolism. Energy metabolism can be studied in the living brain using ^{13}C MRS during administration of ^{13}C-enriched substrates (Henry et al., 2006). By measuring ^{13}C isotope incorporation over time into specific carbon positions of different molecules and by analysing these ^{13}C enrichments over time with appropriate mathematical models, one can determine the rate of oxidative metabolism in

---

SIGNIFICANCE

By quantifying neuronal and glial oxidative metabolism in the living brain under thiopental anaesthesia, we verified a general metabolic depression and further identified that there is an alteration of the relative fraction of glucose oxidation in each cell type, relative to experiments under other anaesthesia protocols, and that substrates other than glucose are substantially used as source of pyruvate for oxidative metabolism.

---

neurons and astrocytes, as well as the glutamate–glutamine cycle rate (e.g., Gruetter et al., 2001; Duarte et al., 2011; Sonnay et al., 2016).

In ^{13}C MRS studies *in vivo*, pentobarbital was administered to induce isoelectricity, allowing baseline metabolic rates to be estimated at a low neurotransmitter turnover (Choi et al., 2002; Chowdhury et al., 2014).

It has been reported that astrocytic glutamate uptake is inhibited by the thiobarbiturates thiopental and thiamylal, but not by oxibarbiturates, including pentobarbital, secobarbital, and amobarbital (Swanson and Seid, 1998). This suggests that thio- and oxibarbiturates have different effects on astrocytic metabolism. The aim of the present study was to investigate neuronal and glial metabolism in the rat cerebral cortex under thiopental anaesthesia using ^{13}C MRS at high magnetic field upon administration of [1,6-^{13}C]glucose.

MATERIALS AND METHODS

Animal Preparation for ^{13}C MRS

All experiments involving animals were performed in accordance with the Swiss federal law on animal experimentation, approved by the local committee (EXPANIM-SCAV), and reported following ARRIVE guidelines. [1,6-^{13}C]glucose (99% [13]C enrichment in both C1 and C6) and other reagents were purchased from Sigma-Aldrich, except where noted. Male Sprague-Dawley rats (n = 7, 267 ± 23 g, from Charles River Laboratoires) were prepared as previously detailed (Duarte et al., 2009). Rats were briefly intubated under 2% isoflurane anaesthesia vaporized in 30% O_2 in air and mechanically ventilated. Catheters were inserted into both femoral veins and one femoral artery. The venal catheters were used for infusion of phosphate-buffered saline solutions containing [1,6-^{13}C]glucose, (RS)-(5-ethyl-4,6-dioxo-5-[pentan-2-yl]-1,4,5,6-tetrahydropyrimidin-2-yl)sulfanide sodium (sodium thiopental, Inresa Arzneimittel), or sodium bicarbonate. The arterial catheter served to collect blood samples, and monitor heart rate and arterial blood pressure. The rat's head was stereotaxically fixed in a homebuilt MR-compatible holder, and the radiofrequency coil was placed on top of the head. Body temperature was maintained at 37 °C with a warm water circulation system based on the feedback obtained from a homebuilt rectal temperature probe. Heart rate, blood pressure and breathing rate were continuously recorded with a SA Instruments monitoring system.

Arterial pH and pressures of CO_2 (P_aCO_2) and O_2 (P_aO_2) were measured with a blood gas analyser (AVL Compact 3, Roche), and were adjusted by regulating both the respiratory rate and volume, and by infusion of $NaHCO_3$ (0.45 M

in saline) to a maximal dose of 3 mmol/kg/h. Plasma glucose was determined with a Reflotron Plus system (Roche). Lactate concentrations were measured with a GM7 Micro-Stat analyser (Analox Instruments).

Once the animal was placed in the scanner, thiopental (10 g/L in saline) was administered as a 50 mg/kg bolus during 5 minutes while isoflurane anaesthesia was discontinued, and then maintained at a continuous infusion rate of 90 mg/kg/h. As previously observed (Duarte and Gruetter, 2012), the high dose of thiopental led to a decrease in heart rate and arterial blood pressure. Once heart rate and blood pressure were stable, about two hours after the thiopental bolus, [1,6-^{13}C]glucose was infused to reach 70% of fractional enrichment (FE) in plasma within 5 minutes and throughout the entire experiment, as described previously (Duarte et al., 2011).

MRS Experiments

All experiments were performed on a 14.1 T/26 cm horizontal bore magnet (Magnex Scientific), equipped with 12 cm gradients (400 mT/m in 120 μs) and interfaced to a direct drive console (Agilent Technologies) using a homebuilt ^{1}H quadrature surface coil combined with a ^{13}C linearly polarized surface coil. T_2-weighted fast-spin-echo images were used for visualisation of anatomical landmarks and placement of a volume of interest (VOI) in the cortex comparable to that of a previous study ($2.2 \times 8.5 \times 5$ mm^3, Sonnay et al., 2016). The static magnetic field was homogenized by FAST(EST)MAP shimming (Gruetter and Tkác, 2000). Amino acid concentrations were measured by ^{1}H MRS using STEAM with repetition time of 4 s, echo time of 2.8 ms, and mixing time of 20 ms. ^{13}C MRS was performed using semi-adiabatic distortionless enhancement by polarization transfer (DEPT) combined with 3D-ISIS ^{1}H localization (Henry et al., 2003a). LCModel (Stephen Provencher Inc.) was used to analyse both ^{1}H and ^{13}C spectra (Henry et al., 2003b).

After MRS experiment, rats were sacrificed with a focused microwave fixation device irradiating the brain for 2.2 s at 4 kW and 2.45 GHz (Gerling Applied Engineering), and the portion of cortex corresponding to the MRS VOI was dissected. Samples of cortex and plasma were immediately stored at -80 °C until further processing. Water-soluble metabolites were extracted with 7% (v/v) perchloric acid. Samples were then lyophilized, re-dissolved in ^2H_2O (99.9% ^2H, Sigma-Aldrich) and the p^2H was adjusted to 7.0 with ^2HCL or NaO^2H. Fully relaxed ^{1}H and ^{13}C MRS *in vitro* were performed as previously detailed (Duarte et al., 2007) on a DRX-600 spectrometer equipped with a 5-mm cryoprobe (Bruker BioSpin SA). FE of glutamate C3 was estimated from ^{13}C spectra of extracts by calculating C4D34/(C4S + C4D34), where C4D34 and C4S are, respectively, the doublet and singlet in the resonance of C4 from glutamate (Duarte and Gruetter, 2013). Note that the total C4 signal corresponds to C4S + C4D34 because glutamate C5 does not become labelled upon administration of [1,6-^{13}C]glucose (Duarte et al., 2011). Labelling of glutamate C3 was then used to calculate labelling in other resonances of the ^{13}C spectra, which served to scale ^{13}C curves measured *in vivo*.

Data Analyses

The analyses of data from ^{13}C MRS experiments in the cortex were performed as described previously (Sonnay et al., 2016), employing the mathematical model of brain energy metabolism (supplementary information) previously detailed (Duarte et al., 2011). Briefly, glucose transport was analysed with a reversible Michaelis-Menten model using both steady state and dynamic MRS data (Duarte and Gruetter, 2012). Steady-state analysis of glucose concentrations measured in cortex and plasma were used to estimate the apparent Michaelis constant of glucose transport K_t. This value was then constrained in the fitting of dynamic ^{13}C curves, determining therefore the apparent maximum transport rate (T_{max}) and the cerebral metabolic rate of glucose (CMR_{glc}). The two-compartment model of energy metabolism (Duarte et al., 2011) was fitted to the group average ^{13}C enrichment curves of all aliphatic carbons of glutamate, glutamine and aspartate. Concentrations of amino acids were assumed not to vary during infusion of [1,6-^{13}C]glucose, and were set as total metabolic pool sizes in the modelling process. The determined parameters included fluxes through the apparent glutamate-glutamine cycle (V_{NT}), neuronal and glial TCA cycles (V_{TCA}^n and V_{TCA}^g), exchange between TCA cycle intermediates oxaloacetate and 2-oxoglutarate with the respective amino acids (V_X^n in neurons and V_X^g in glia), pyruvate carboxylase (V_{PC}), as well as dilution fluxes at the level of pyruvate (V_{in}, V_{out}), glial acetyl-CoA (V_{dil}), and glial glutamine (V_{ex}^g). Calculated fluxes comprised the fraction of the glial TCA cycle that results in full oxidation of pyruvate ($V_g = V_{TCA}^g - V_{PC}$), the glutamine synthetase rate ($V_{GS} = V_{NT} + V_{PC}$) and the total rate of oxidative glucose metabolism, that is $CMR_{glc(ox)} = (V_{TCA}^n + V_{TCA}^g + V_{PC})/2$.

All data are shown as mean and standard deviation (SD). For metabolic fluxes, the SD of each parameter was estimated from fitting a Gamma function to the probability distribution that resulted from 2000 simulations in a Monte-Carlo analysis (Duarte et al., 2011; Sonnay et al., 2016). Calculated fluxes include error propagation in their SD.

A permutation analysis, with 2000 random permutations followed by individual two-tailed student t-tests, was employed to compare measured metabolic fluxes to those reported previously (Sonnay et al., 2016) under identical conditions but with α-chloralose anaesthesia. P-values were corrected for multiple comparisons, and significance was considered for $P < 0.05$.

RESULTS

To achieve stable FE during the ^{13}C MRS experiment, [1,6-^{13}C]glucose was infused, which resulted in an increase of plasma glucose concentration (Fig. 1). At the end of the experiment, FE of glucose C1 was $67 \pm 3\%$ in plasma and $66 \pm 3\%$ in brain extracts. Administration of [1,6-^{13}C]glucose under thiopental anaesthesia increased plasma lactate concentration (Fig. 1) to 5.7 ± 1.4 mM during the last hour of [1,6-^{13}C]glucose administration. FE of lactate C3 reached $49 \pm 3\%$ in plasma and $57 \pm 7\%$ in cortex at the end of the experiment. In addition to lactate, plasma alanine and acetate became enriched, although their respective concentrations were below 1 mM and did not change during glucose infusion. At the
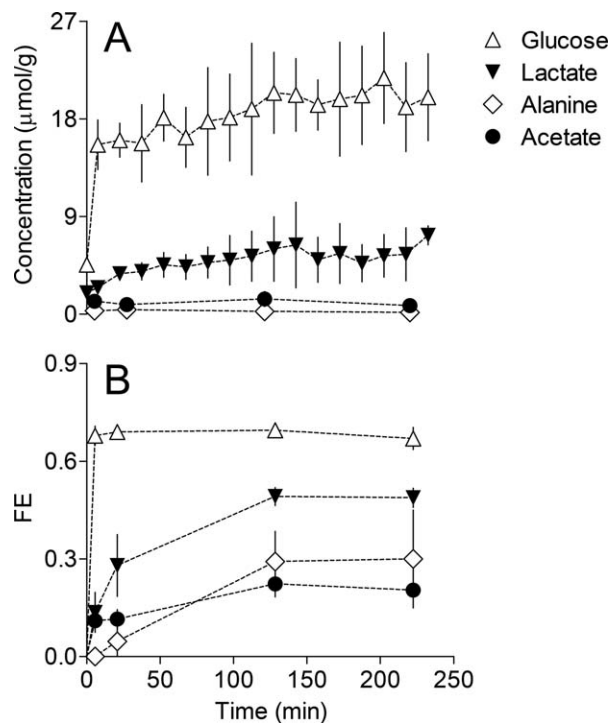

Fig. 1. Plasma concentrations and fractional enrichment (FE) of glucose, lactate, alanine, and acetate. Concentrations of glucose and lactate were measured along the experiment *in vivo*. FE of metabolites and concentrations of alanine and acetate were quantified in plasma extracts by MRS *in vitro*.

end of the experiment, the FE of alanine C3 and acetate C2 was $30 \pm 26\%$ and $20 \pm 4\%$ in plasma, and $52 \pm 2\%$ and $2 \pm 3\%$ in cortical extracts, respectively. Note that blood physiology was maintained within normal limit under thiopental anaesthesia. Namely, P_aCO_2 was 42.2 ± 3.4 mm Hg, pH was 7.35 ± 0.05 and O_2 saturation was $99.6 \pm 0.2\%$. Average heart rate was 281 ± 51 bpm, and systolic and diastolic blood pressures were 140 ± 11 and 85 ± 19 mm Hg, respectively.

Overall quality of ^{13}C spectra was similar to our previous study performed in the rat cortex under α-chloralose (Sonnay et al., 2016), with well-resolved peaks for glucose C1 and C6, and all the aliphatic carbons of glutamate, glutamine and aspartate at a temporal resolution of 10.6 minutes (Fig. 2).

To assess transport kinetics of glucose across the blood-brain-barrier, brain and plasma glucose concentrations were measured at steady state (Fig. 3A) and evaluated using reversible Michaelis-Menten modelling, which resulted in a K_t of 4.5 ± 5.6 mM and a T_{max}/CMR_{glc} of 7.8 ± 3.7. To obtain an estimate of T_{max} and CMR_{glc}, dynamic analysis of glucose transport and consumption was made on glucose enrichment during the first hour of infusion, since the largest glucose variations occur at the onset of glucose administration (Fig. 3B). Analysis of dynamic enrichment of brain glucose upon infusion of [1,6-^{13}C]glucose with K_t constrained to 4.5 mM resulted
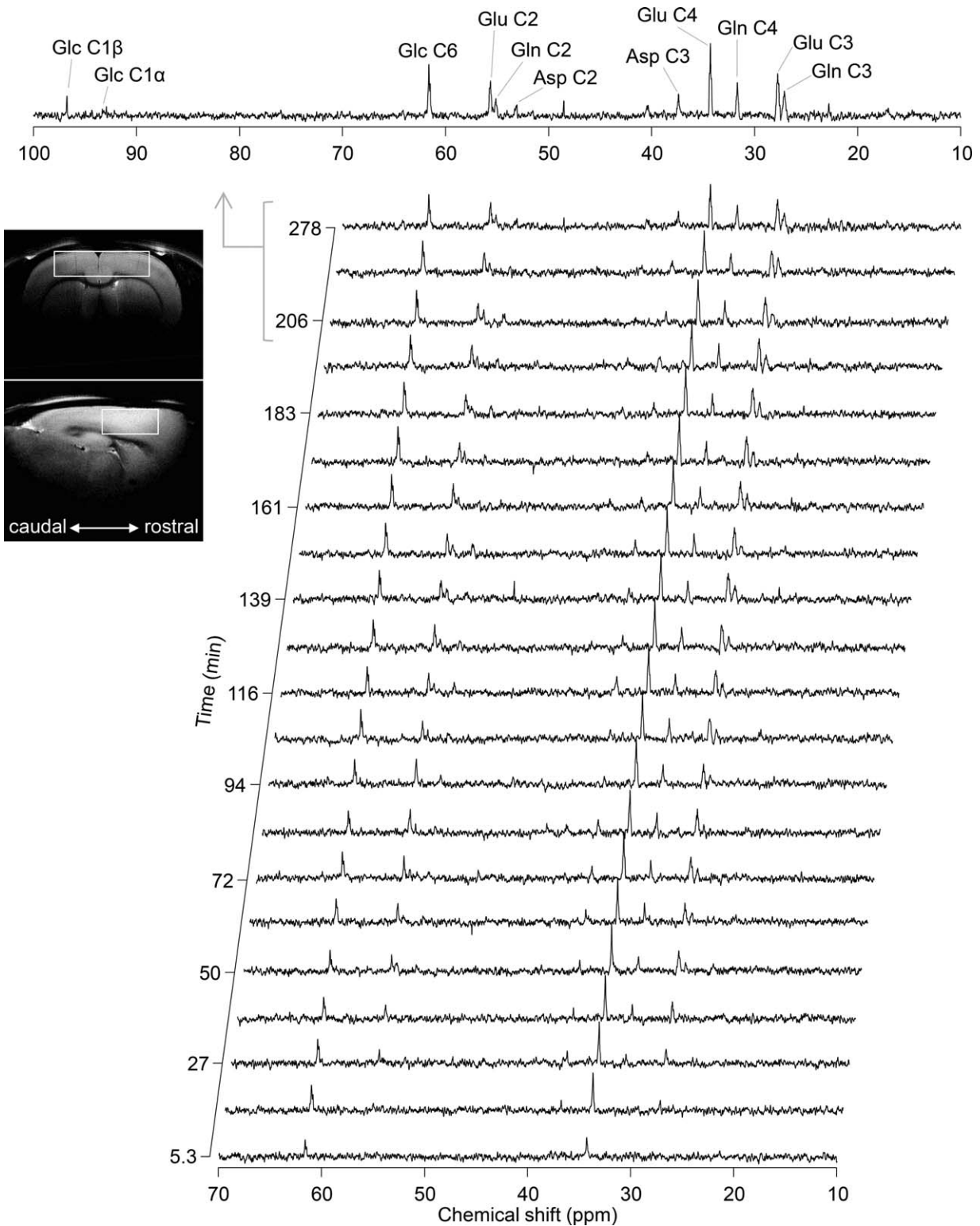
Fig. 2. Typical ^{13}C spectra acquired at 14.1 T from a volume of 94 μL in the rat cortex during [1,6-^{13}C]glucose infusion under thiopental anaesthesia. Spectra are shown with a temporal resolution of 10.6 minutes, starting from the [1,6-^{13}C]glucose administration (t = 0). A time scale for this particular experiment is shown along the spectra. The top spectrum is the sum of the last 3 spectra. Lorentzian apodization (7 Hz) was applied prior to Fourier transformation. Peak assignment: Glc, glucose; Glu, glutamate; Gln, glutamine; Asp, aspartate. The coronal and sagittal images of the rat brain show the precise VOI location in the rat cortex.
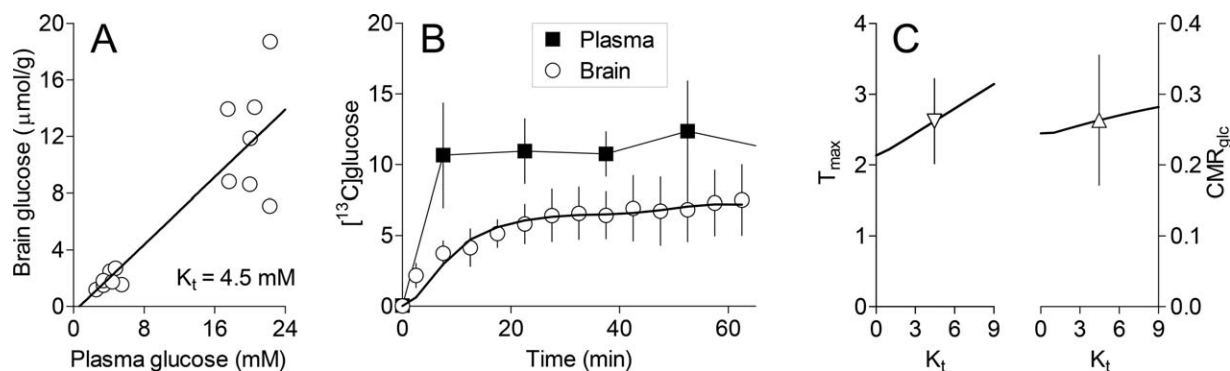
Fig. 3. Glucose transport and consumption in the rat cortex. **(A)** Description of plasma and cortical glucose concentrations at steady-state by the reversible Michaelis-Menten model for determination of K_t. Cortical glucose concentrations at glycaemia below 8 mM were measured by ^{1}H MRS *in vivo* before [1,6-^{13}C]glucose infusion. At plasma glucose above 16 mM, cortical glucose concentrations were calculated from the FE in cortical extracts and the average [^{13}C]glucose measured *in vivo* by ^{13}C MRS during the last 30 minutes of experiment. **(B)** Dynamic analysis of brain glucose transport and consumption using brain [^{13}C]glucose (in µmol/g, open symbols) and plasma [^{13}C]glucose (in mM, filled symbols) during the first hour of glucose infusion, when cortical glucose changes the most. Plasma [^{13}C]glucose was estimated from total glucose concentration and the FE measured in plasma extracts. Cortical [^{13}C]glucose was directly measured by ^{13}C MRS *in vivo*. The best fit of the model is represented by the solid line over the [^{13}C]glucose time course in the cortex. **(C)** Analysis of the effect of K_t (in mM) on the determination of T_{max} and CMR_{glc} (both in µmol/g/min).

in $T_{max} = 2.6 \pm 0.6$ µmol/g/min and $CMR_{glc} = 0.26 \pm 0.09$ µmol/g/min. Although there was a large uncertainty associated to K_t, this parameter was devoid of major effects on the estimation of T_{max} and CMR_{glc}. Namely, changing K_t from 0 to 9 mM resulted in T_{max} and CMR_{glc} variations within their SD (Fig. 3C). In turn, CMR_{glc} was devoid of effect on the fluxes of neuronal and glial metabolism, excepting the estimation of V_{in} and V_{out}.

Concentrations of glutamate, glutamine and aspartate in the rat cortex under thiopental anaesthesia were 10.8 ± 0.9, 4.8 ± 1.4, and 3.5 ± 0.7 µmol/g, respectively, and used as metabolic pool sizes in the model. To obtain metabolic rates, the two-compartment model of energy metabolism (Duarte et al., 2011; Sonnay et al., 2016) was fitted to the experimentally measured ^{13}C turnover curves ($R^2 = 0.968$, Fig. 4A), and uncertainty of estimated parameters was assessed by Monte-Carlo analysis (Fig. 5). The rate of glutamatergic neurotransmission, i.e., the glutamate-glutamine cycle (V_{NT}), was 0.09 ± 0.02 µmol/g/min and glutamine synthetase (V_{GS}) was 0.12 ± 0.01 µmol/g/min. The fluxes through the tricarboxylic acid cycles in neurons (V_{TCA}^n) and in astrocytes (V_{TCA}^g) were 0.46 ± 0.02 and 0.16 ± 0.02 µmol/g/min, respectively. Pyruvate carboxylation (V_{PC}) was 0.02 ± 0.01 µmol/g/min, representing 15% of V_{TCA}^g. In turn, V_{TCA}^g was about one fourth of total cortical glucose oxidative metabolism, which is $CMR_{glc(ox)} = 0.32 \pm 0.01$ µmol/g/min. In the present experiments, estimation of V_X^n and V_X^g resulted in variances two orders of magnitude larger than the estimated value ($V_X^n = 5.79 \pm 3.92$ µmol/g/min; $V_X^g = 3.45 \pm 2.84$ µmol/g/min; see Table I). To assess the influence of experimental noise on the estimated metabolic rates, Monte-Carlo simulations were performed and the histograms analysed. The uncertainty of the exchange fluxes (V_X^n and V_X^g) does not preclude the utilisation of the model for estimating the remaining fluxes of oxidative metabolism, which displayed a nearly Gaussian distribution (Fig. 5). The dilution of acetyl-CoA (V_{dil}) approached zero in the fitting and in all Monte-Carlo simulations, as previously observed in the rat cortex under α-chloralose anaesthesia (Sonnay et al., 2016). Interestingly, in the present study, $CMR_{glc(ox)}$ was larger than the glycolytic rate (0.32 ± 0.01 *vs.* 0.26 ± 0.09 µmol/g/min). Therefore, there was no loss of pyruvate (V_{out}) but rather a net influx of pyruvate molecules at 0.12 ± 0.09 µmol/g/min (V_{in}-V_{out}), most probably from lactate.

The results obtained under thiopental anaesthesia in this study were compared with those acquired in similar experimental conditions but under α-chloralose anaesthesia (Fig. 4B) in a previous study, also in the rat cortex (Sonnay et al., 2016). When compared to α-chloralose (Table I), thiopental anaesthesia inhibited CMR_{glc} (-45%), $CMR_{glc(ox)}$ (-29%), V_{TCA}^n (-13%), V_g (-42%), V_{PC} (-67%), and V_{TCA}^g (-48%).

DISCUSSION

The present study *in vivo* quantifies for the first time the relative contribution of neurons and astrocytes under thiopental anaesthesia, and demonstrates that there is a depression of neuronal and astrocytic metabolism (depicted by V_{TCA}^n, V_{TCA}^g and V_{PC}) under such conditions, and an important alteration in the relative fraction of glucose that is oxidised in each cell type, when compared to identical experiments under light α-chloralose anaesthesia (Sonnay et al., 2016), as well as to awake rats (Oz et al., 2004). Namely, while oxidative metabolism was about 60% in neurons and 40% in astrocytes both in conscious rats (Oz et al., 2004) and in rats under α-chloralose anaesthesia (Duarte et al., 2011; Sonnay
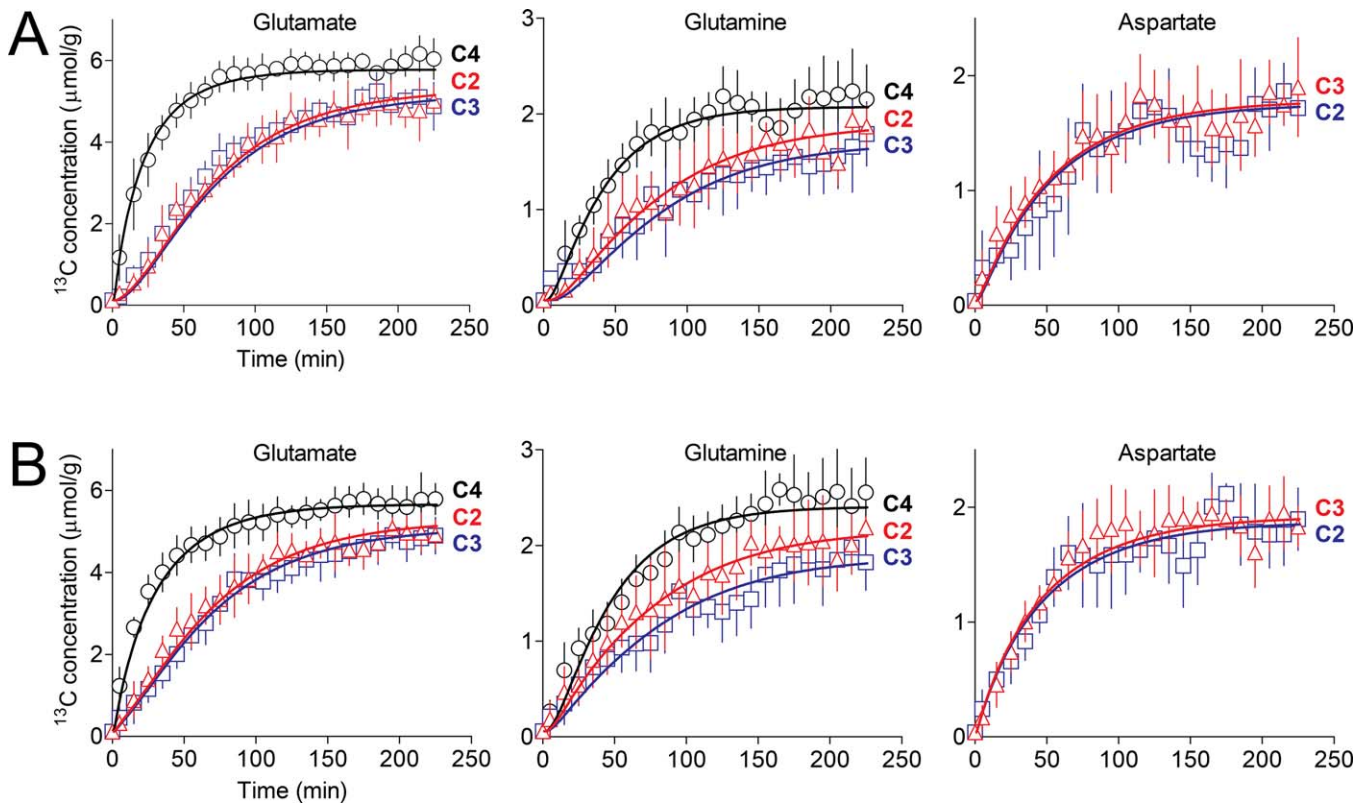
Fig. 4. Average ^{13}C enrichment curves (in µmol/g) of aliphatic carbons of glutamate (Glu), glutamine (Gln) and aspartate (Asp) measured in the rat cortex, and best fit (solid lines) of the two-compartment model of brain energy metabolism. Experiments under thiopental (current study) and α-chloralose (Sonnay et al., 2016) anaesthesia are shown in panels A and B, respectively. For glutamate and glutamine, ^{13}C concentration in carbons 4, 3, and 2 are depicted by circles, squares, and triangles, respectively. For aspartate, triangles and squares are the ^{13}C concentration in C3 and C2, respectively.

et al., 2016), astrocytes contributed with only 28% to whole cortical oxidative metabolism under thiopental. This is consistent with previous cell culture studies showing larger reduction of glucose uptake in astrocytes (Qu et al., 1999) than in neurons (Qu et al., 2000).

Barbiturates generally depress cerebral activity and thus reduce the rate of glucose utilisation (Hodes et al., 1985; Nilsson and Siesjo, 1975; Sokoloff et al., 1977; Strang and Bachelard, 1973; Crane et al., 1978), as well as the rate of oxidative metabolism in both neurons and astrocytes (Weiss et al., 1972; Hertz et al., 1986; Yu et al., 1983; Qu et al., 1999, 2000). Namely, employing a methodology similar to that of our study, Oz et al., (2014) investigated brain energy metabolism in the whole brain of the awake rat and found V_{TCA}^n, V_{TCA}^g and V_{PC} of 1.13 ± 0.14, 0.54 ± 0.09, and 0.14 ± 0.03 µmol/g/min, respectively. Relative to this study, thiopental anaesthesia reduced V_{TCA}^n by about 60%, V_{TCA}^g by 70%, and V_{PC} by 80%. Moreover, cell-permeant barbiturates directly depress mitochondrial respiration (e.g., Aldridge and Parker, 1960; Chance and Hollunger, 1963), and thereby cause mitochondrial depolarisation and deregulation of Ca^{2+} homeostasis, resulting in energy depletion that can eventually facilitate NMDA-induced neurotoxicity (Anderson et al., 2002). Notably, the brain concentration of thiopental that was likely achieved in the present study (Harashima et al., 1997) is in the range that effectively causes the aforementioned effects in cultured neurons (30-100 µM, Anderson et al., 2002). However, with this thiopental dose, we did not find a reduction of phosphocreatine-to-creatine ratio in the rat brain (Duarte and Gruetter, 2012) and cortex (Lei et al., 2010), suggesting that the energy status is well preserved in the living rat brain.

Thiopental was administered at a dose capable of inducing isoelectricity in the rat brain (Gustafsson et al., 1996; Harashima et al., 1997). To our surprise, the rate of the glutamate-glutamine cycle (depicted by V_{NT}) was similar in experiments performed under thiopental (present study) and α-chloralose anaesthesia (Sonnay et al., 2016), although much smaller than that reported in cortical areas or the whole brain of the awake rat (Oz et al., 2004; Wang et al., 2010). In contrast, ^{13}C MRS experiments in the whole rat brain found that V_{NT} under pentobarbital anaesthesia (Choi et al., 2002) is less than half of that under α-chloralose anaesthesia (Duarte et al., 2011).
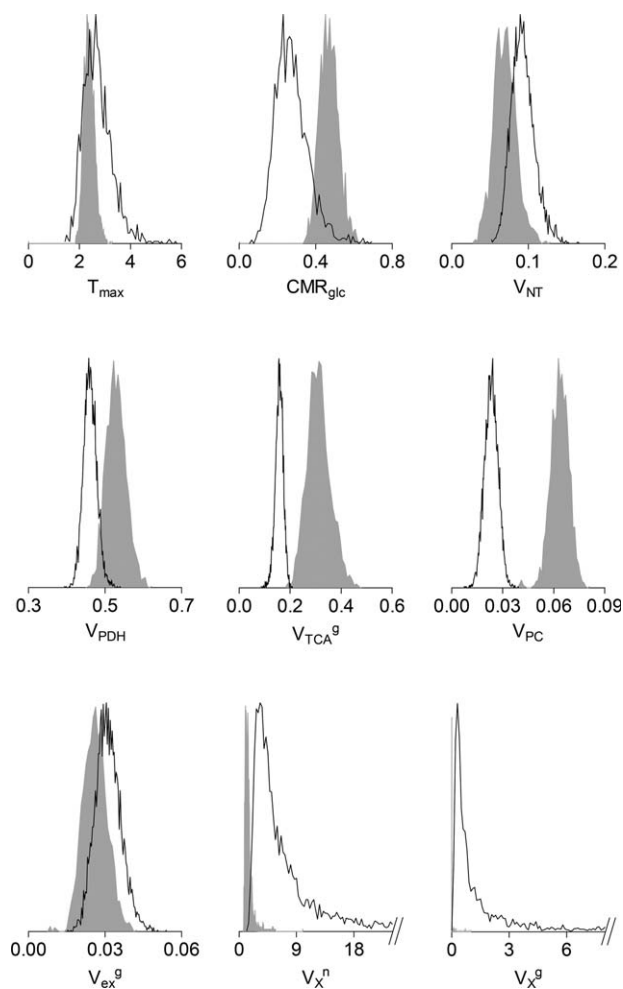
Fig. 5. Probability distribution resulting from the Monte-Carlo analysis of the measured metabolic fluxes in the rat cortex under thiopental (line) and α-chloralose anesthesia (shaded area).

TABLE I. Metabolic Fluxes (in μmol/g/min) in the Rat Cortex Under Thiopental Anaesthesia Compared to Those Under α-chloralose Anaesthesia Previously Reported in (Sonnay et al., 2016). Fluxes were Compared with Independent Student t-tests in a Permutation Analysis ($\star P < 0.05$ After Correction for Multiple Testing).

Anaesthesia	thiopental (n = 7)	α-chloralose (n = 8)
Measured fluxes:		
T_{max}	2.62 ± 0.60	2.38 ± 0.26
CMR_{glc}	0.26 ± 0.09	$0.47 \pm 0.05\star$
V_{NT}	0.09 ± 0.02	0.07 ± 0.01
V_{TCA}^{n}	0.46 ± 0.02	$0.53 \pm 0.02\star$
V_{g}	0.13 ± 0.02	$0.24 \pm 0.04\star$
V_{PC}	0.02 ± 0.01	$0.06 \pm 0.01\star$
V_{X}^{n}	$5.79 \pm 3.92^{\S}$	1.28 ± 0.43
V_{X}^{g}	$3.45 \pm 2.84^{\S}$	0.01 ± 0.03
V_{in}	0.12 ± 0.09	0.17 ± 0.02
V_{dil}	–	–
V_{ex}^{g}	0.03 ± 0.01	0.03 ± 0.01
Calculated fluxes:		
V_{GS}	0.12 ± 0.01	0.13 ± 0.02
V_{out}	–	$0.20 \pm 0.08\star$
V_{TCA}^{g}	0.16 ± 0.02	$0.31 \pm 0.02\star$
$CMR_{glc(ox)}$	0.32 ± 0.01	$0.45 \pm 0.03\star$

§Given the long tail of V_{X} histograms, SD calculation for V_{X}^{n} and V_{X}^{g} in thiopental experiments excluded values in the histogram above a threshold of 20 μmol/g/min. In this case, the number of Monte-Carlo simulations used was 1613 for V_{X}^{n} and 1160 for V_{X}^{g}.

This indicates that the tight coupling between energy metabolism and glutamatergic neurotransmission or glutamate-glutamine cycle (e.g., Hyder and Rothman, 2012; Lanz et al., 2013) is not maintained under thiopental anaesthesia. Therefore, one may speculate that the modulation of neurotransmitter homeostasis by thiopental might involve different TCA cycle-mediating effects, such as production of amino acids (Qu et al., 2000). Since the energy requirements directly linked to the glutamate-glutamine cycle (e.g. Na^{+}/K^{+} ATPase extrusion of Na^{+} that is co-transported with glutamate, glutamine synthetase activity, glutamate transport into vesicles) are relatively small compared to the total energy produced (at the ATP rates estimated in the present study), the relatively high metabolic rates measured under thiopental anaesthesia (compared to pentobarbital) must be required to support other processes involved in neurotransmission, namely stabilization of the membrane potentials or post-synaptic ion influxes (Attwell et al., 2001).

Similar to other barbiturates, inhibition of stimulation-induced release of GABA, aspartate, glutamate and/or dopamine by thiopental was demonstrated in rat cerebrocortical slices (Minchin, 1981; Buggy et al., 2000), cultured cerebellar neurons (Qu et al., 2000), and synaptosomes (Pastuszko et al., 1984; Mantz et al., 1994; Lecharny et al., 1995). In contrast to the release of neurotransmitters, their re-uptake is not equally modulated by all barbiturates. Thiopental does not affect glutamate and aspartate uptake in cerebellar neurons in culture (Qu et al., 2000). In rat brain synaptosomes, thiopental does not affect glutamate and GABA uptake (Sugimura et al., 2001), although it can inhibit uptake of dopamine (Keita et al., 1996). In a comparative study, Minchin (1981) reported that pentobarbital could inhibit GABA and aspartate uptake by nerve terminals, while thiopental was devoid of effect on amino acid uptake (as well as α-chloralose, which we employed in a past study, Sonnay et al., 2016). In contrast to these studies, others reported that thiopental inhibits synaptosomal uptake of aspartate, GABA and dopamine (Pastuszko et al., 1984; Mantz et al., 1995). To summarize, thiopental inhibits the release of neurotransmitters and, only in certain conditions, also their reuptake by neurons. Interestingly, thiopental was also shown to inhibit neuronal catabolism of glutamate (Qu et al., 2000) and GABA (Cheng and Brunner, 1981), which may be due to the inhibition of neuronal oxidative metabolism.

Interestingly, in cortical astrocytes in culture, thiopental inhibits glutamate uptake (Swanson and Seid, 1998). Qu et al. (1999) further reported thiopental-induced inhibition of astrocytic glutamate metabolism through the TCA cycle. In contrast, pentobarbital (as other oxibarbiturates) is devoid of effect on glutamate transport in astrocytes cultured from either the cortex (Swanson and Seid, 1998) or the hippocampus (Miyzaki et al., 1997). Glutamate uptake is an energy-dependent process. Accordingly, in the present study, only 25% of cortical glucose oxidation, that is $CMR_{glc(ox)}$, occurred in astrocytes, while it was nearly 40% under light α-chloralose anaesthesia in either the rat cortex (Sonnay et al., 2016) or the whole brain (Duarte et al., 2011; Duarte and Gruetter, 2013; Lanz et al., 2014; Dehghani et al., 2016). Furthermore, impaired clearance of synaptic glutamate in the living brain under thiopental anaesthesia likely results in enhanced neuronal activity and neuronal oxidative metabolism. In fact, thiopental but not pentobarbital was shown to produce spontaneous repetitive action potentials in the squid giant axon, likely due to the higher affinity of thiopental to potassium channels resulting in the prolongation of the falling phase of action potentials (Sevcik, 1980). This may explain the relatively high rate of labelling incorporation from $[1,6-^{13}C]$glucose into amino acids, namely when compared to pentobarbital experiments (Choi et al., 2002). Likewise, in the present experiments in the living brain, V_{GS} was similar to that estimated under light α-chloralose anaesthesia. Regarding the ability of thiopental to inhibit glutamine production, there have been contrasting reports. Namely, while Qu et al. (1999) suggested that glutamine synthesis and release could be inhibited by thiopental in cultured astrocytes, an earlier study found no effect (Yu et al., 1983).

The cortical rate of glycolysis (CMR_{glc}) was substantially lower than that estimated under α-chloralose anaesthesia (Sonnay et al., 2016), resulting in considerably reduced glucose consumption relative to its transport capacity at the blood-brain-barrier (Lei et al., 2010; Duarte and Gruetter, 2012), probably due to inhibition of both hexokinase (Bielicki and Krieglstein, 1976) and phosphofructokinase (Carlsson et al., 1975). Interestingly, under thiopental anaesthesia, $CMR_{glc(ox)}$, i.e., the total rate of oxidative metabolism, was estimated to be larger than the glycolytic rate, implying a net influx of other carbon molecules into the acetyl-CoA pool, likely from lactate or acetate. It is noteworthy that infusion of $[1,6-^{13}C]$glucose under thiopental resulted in a nearly two-fold increase in plasma lactate concentration relative to what was observed in experiments under α-chloralose anaesthesia (Duarte et al., 2011, Sonnay et al., 2016). Hyperlactemia likely results in increased utilisation of lactate by the brain owing to the facilitated diffusion mechanism of MCT transporters and, therefore, $[3-^{13}C]$lactate substantially contributes to enrich carbons of cortical amino acids with labelling patterns identical to those of $[1,6-^{13}C]$glucose (e.g., Gallagher et al., 2009; Boumezbeur et al., 2010; Duarte et al., 2015). In the present

experiments with glucose infusion, rather than a net loss of pyruvate molecules as observed under α-chloralose anaesthesia (Duarte et al., 2011; Duarte and Gruetter, 2013; Sonnay et al., 2016), we estimated a net consumption of three-carbon molecules that amounts to one fifth of total mitochondrial metabolism. Therefore, it is likely that lactate was used as an alternate metabolic substrate under thiopental anaesthesia.

We proposed previously (Lanz et al., 2013) that the exchange fluxes, V_X^n and V_X^g, reflecting the malate-aspartate shuttle rate (Gruetter et al., 2001) could be associated to the rate of mitochondrial oxidation in the respective compartment, as this pathway is used for transporting reducing equivalents into mitochondria. In this study, there was a large uncertainty associated to the estimation of the exchange fluxes V_X^n and V_X^g (Table I), precluding a fair comparison to results under α-chloralose anaesthesia (Sonnay et al., 2016). Nevertheless, the magnitude of these fluxes appears to be much larger than that of the respective TCA cycle fluxes under thiopental anaesthesia, as well as larger than under other anaesthesia conditions (summarised in Lanz et al., 2013). Accordingly, increased aspartate-malate shuttle activity was also observed *in vivo* in rats with reduced mitochondrial respiration after treatment with 3-nitropropionic acid, an inhibitor of succinate dehydrogenase (Henry et al., 2002).

Altogether, we conclude that cortical rates of oxidative metabolism in both glia and neurons are lower under thiopental than α-chloralose anaesthesia *in vivo*. They remain nevertheless substantial, as reflected by the relatively high rate of labelling incorporation from $[1,6-^{13}C]$glucose into amino acids. Finally, given the low glycolytic rate relative to neuronal and glial TCA cycle rates, catabolism of other energy substrates is likely to be important in the present experimental conditions.

ACKNOWLEDGEMENTS

CONFLICT OF INTEREST STATEMENT

The authors have no conflicts of interest.

ROLE OF AUTHORS

JMND designed the study, SS performed experiments, all authors contributed to interpreting the data and writing the manuscript. Both SS and JMND had full access to all the data in the study and take responsibility for the integrity of the data and the accuracy of the data analysis.

REFERENCES

Aldridge WN, Parker VH. 1960. Barbiturates and oxidative phosphorylation. Biochem J 76:47-56

Anderson CM, Norquist BA, Vesce S, Nicholls DG, Soine WH, Duan S, Swanson RA. 2002. Barbiturates induce mitochondrial depolarization and potentiate excitotoxic neuronal death. J Neurosci 22(21):9203-9209.

Attwell D, Laughlin SB. 2001. An energy budget for signalling in the grey matter of the brain. J Cereb Blood Flow Metab 21:1133-1145

Bielicki L, Krieglstein J. 1976. Inhibition of glucose phosphorylation in rat brain by thiopental. Naunyn Schmiedebergs Arch Pharmacol 293(1): 25-29.

Boumezbeur F, Petersen KF, Cline GW, Mason GF, Behar KL, Shulman GI, Rothman DL. 2010. The contribution of blood lactate to brain energy metabolism in humans measured by dynamic ^{13}C nuclear magnetic resonance spectroscopy. J Neurosci 30:13983-13991.

Buggy DJ, Nicol B, Rowbotham DJ, Lambert DG. 2000. Effects of intravenous anesthetic agents on glutamate release: a role for GABAA receptor-mediated inhibition. Anesthesiology 92(4):1067-1073.

Carlsson C, Harp JR, Siesjö BK. 1975. Metabolic changes in the cerebral cortex of the rat induced by intravenous pentothalsodium. Acta Anaesthesiol Scand Suppl 57:1-17

Chance B, Hollunger G. 1963. Inhibition of electron and energy transfer in mitochondria. J Biol Chem 278:418-431

Cheng SC, Brunner EA. 1981. Effects of anesthetic agents on synaptosomal GABA disposal. Anesthesiology 55(1):34-40.

Choi IY, Lei H, Gruetter R. 2002. Effect of deep pentobarbital anesthesia on neurotransmitter metabolism in vivo: on the correlation of total glucose consumption with glutamatergic action. J Cereb Blood Flow Metab 22:1343-5110.

Chowdhury GM, Jiang L, Rothman DL, Behar KL. 2014. The contribution of ketone bodies to basal and activity-dependent neuronal oxidation in vivo. J Cereb Blood Flow Metab 34(7):1233-1242.

Crane PD, Braun LD, Cornford EM, Cremer JE, Glass JM, Oldendorf WH. 1978. Dose dependent reduction of glucose utilization by pentobarbital in rat brain. Stroke 9(1):12-18.

Dehghani MM, Lanz B, Duarte JMN, Kunz N, Gruetter R. 2016. Refined analysis of brain energy metabolism using in vivo dynamic enrichment of ^{13}C multiplets. ASN Neuro 8(2):1759091416632342.

Duarte JMN, Carvalho RA, Cunha RA, Gruetter R. 2009. Caffeine consumption attenuates neurochemical modifications in the hippocampus of streptozotocin-induced diabetic rats. J Neurochem 111(2):368-379.

Duarte JMN, Cunha RA, Carvalho RA. 2007. Different metabolism of glutamatergic and GABAergic compartments in superfused hippocampal slices characterized by nuclear magnetic resonance spectroscopy. J Neuroscience 144(4):1305-1313

Duarte JMN, Girault FM, Gruetter R. 2015. Brain energy metabolism measured by 13C magnetic resonance spectroscopy in vivo upon infusion of [3-^{13}C] lactate. J Neurosci Res 93(7):1009-1018

Duarte JMN, Gruetter R. 2012. Characterization of cerebral glucose dynamics in vivo with a four-state conformational model of transport at the blood-brain barrier. J Neurochem 121(3):396-406.

Duarte JMN, Gruetter R. 2013. Glutamatergic and GABAergic energy metabolism measured in the rat brain by ^{13}C NMR spectroscopy at 14.1 T. J Neurochem 126(5):579-590.

Duarte JMN, Lanz B, Gruetter R. 2011. Compartmentalized cerebral metabolism of [1,6-^{13}C]glucose determined by in vivo ^{13}C NMR spectroscopy at 14.1 T. Front Neuroenergetics 3:3.

Gallagher CN, Carpenter KL, Grice P, Howe DJ, Mason A, Timofeev I, Menon DK, Kirkpatrick PJ, Pickard JD, Sutherland GR, Hutchinson PJ. 2009. The human brain utilizes lactate via the tricarboxylic acid cycle: a ^{13}C-labelled microdialysis and high-resolution nuclear magnetic resonance study. Brain 132:2839-2849.

Gruetter R, Seaquist ER, Ugurbil K. 2001. A mathematical model of compartmentalized neurotransmitter metabolism in the human brain. Am J Physiol Endocrinol Metab 281(1):E100-E112.

Gruetter R, Tkác I. 2000. Field mapping without reference scan using asymmetric echo-planar techniques. Magn Reson Med 43(2):319-323.

Gustafsson LL, Ebling WF, Osaki E, Stanski DR. 1996. Quantitation of depth of thiopental anesthesia in the rat. Anesthesiology 84(2):415-427.

Harashima H, Ebling WF, Wada DR, Stanski DR. 1997. No effect of age on the dose requirement of thiopental in the rat. Exp Gerontol 32(3):315-324.

Henry PG, Lebon V, Vaufrey F, Brouillet E, Hantraye P, Bloch G. 2002. Decreased TCA cycle rate in the rat brain after acute 3-NP treatment measured by in vivo ^{1}H-[^{13}C] NMR spectroscopy. J Neurochem 82(4):857-866.

Henry PG, Oz G, Provencher S, Gruetter R. 2003b. Toward dynamic isotopomer analysis in the rat brain in vivo: automatic quantitation of ^{13}C NMR spectra using LCModel. NMR Biomed 16(6-7):400-412.

Henry PG, Tkác I, Gruetter R. 2003a. ^{1}H-localized broadband ^{13}C NMR spectroscopy of the rat brain in vivo at 9.4 T. Magn Reson Med 50(4):684-692.

Henry PG, Adriany G, Deelchand D, Gruetter R, Marjanska M, Oz G, Seaquist ER, Shestov A, Ugurbil K, In vivo 13C NMR spectroscopy and metabolic modeling in the brain: a practical perspective. Magn Reson Imag 24(4):527-539.

Hertz E, Shargool M, Hertz L. 1986. Effects of barbiturates on energy metabolism by cultured astrocytes and neurons in the presence of normal and elevated concentrations of potassium. Neuropharmacology 25(5):533-539.

Hertz L, Peng L, Dienel GA. 2007. Energy metabolism in astrocytes: High rate of oxidative metabolism and spatiotemporal dependence on glycolysis/glycogennolysis. J Cereb Blood Flow Metab 27:219-249.

Hodes JE, Soncrant TT, Larson DM, Carlson SG, Rapoport SI. 1985. Selective changes in local cerebral glucose utilization induced by phenobarbital in the rat. Anesthesiology 63:633-639

Hyder F, Rothman DL. 2012 Quantitative fMRI and oxidative neuroenergetics. Neuroimage 62(2):985-994.

Ito T, Suzuki T, Wellman SE, Ho IK. 1996. Pharmacology of barbiturate tolerance/dependence: GABAA receptors and molecular aspects. Life Sci 59(3):169-195.

Keita H, Lecharny JB, Henzel D, Desmonts JM, Mantz J. 1996. Is inhibition of dopamine uptake relevant to the hypnotic action of i.v. anaesthetics? Br J Anaesth 77(2):254-256.

Lanz B, Gruetter R, Duarte JMN. 2013. Metabolic flux and compartmentation analysis in the brain in vivo. Front Endocrinol (Lausanne) 4: 156

Lanz B, Xin L, Millet P, Gruetter R. 2014. In vivo quantification of neuro-glial metabolism and glial glutamate concentration using ^{1}H-[^{13}C] MRS at 14.1T. J Neurochem 128:125-139

Lecharny JB, Salord F, Henzel D, Desmonts JM, Mantz J. 1995. Effects of thiopental, halothane and isoflurane on the calcium-dependent and -independent release of GABA from striatal synaptosomes in the rat. Brain Res 670(2):308-312.

Lei H, Duarte JMN, Mlynarik V, Python A, Gruetter R. 2010. Deep thiopental anesthesia alters steady-state glucose homeostasis but not the neurochemical profile of rat cortex. J Neurosci Res 88(2):413-419

Mantz J, Lecharny JB, Laudenbach V, Henzel D, Peytavin G, Desmonts JM. 1995. Anesthetics affect the uptake but not the depolarization-evoked release of GABA in rat striatal synaptosomes. Anesthesiology 82(2):502-511.

Mantz J, Varlet C, Lecharny JB, Henzel D, Lenot P, Desmonts JM. 1994. Effects of volatile anesthetics, thiopental, and ketamine on spontaneous and depolarization-evoked dopamine release from striatal synaptosomes in the rat. Anesthesiology 80(2):352-363.

Masamoto K, Kanno I. 2012. Anesthesia and the quantitative evaluation of neurovascular coupling. J Cereb Blood Flow Metab 32(7):1233-1247.

Minchin MC. 1981. The effect of anaesthetics on the uptake and release of gamma-aminobutyrate and D-aspartate in rat brain slices. Br J Pharmacol 73(3):681-689.

Miyazaki H, Nakamura Y, Arai T, Kataoka K. 1997. Increase of glutamate uptake in astrocytes: a possible mechanism of action of volatile anesthetics. Anesthesiology 86(6):1359-1366.

Nilsson L, Siesjo BK. 1975. The effect of phenobarbitone anaesthesia on blood flow and oxygen consumption in the rat brain. Acta Anesthesiol Scand Suppl 57:18-24.

Oz G, Berkich DA, Henry PG, Xu Y, LaNoue K, Hutson SM, Gruetter R. 2004. Neuroglial metabolism in the awake rat brain: CO_2 fixation increases with brain activity. J Neurosci, 24(50):11273-11279.

Pastuszko A, Wilson DF, Erecińska M. 1984. Amino acid neurotransmitters in the CNS: effect of thiopental. FEBS Lett 177(2):249-254.

Qu H, Faerø E, Jørgensen P, Dale O, Gisvold SE, Unsgård G, Sonnewald U. 1999. Decreased glutamate metabolism in cultured astrocytes in the presence of thiopental. Biochem Pharmacol 58(6):1075-1080.

Qu H, Waagepetersen HS, van Hengel M, Wolt S, Dale O, Unsgård G, Sletvold O, Schousboe A, Sonnewald U. 2000. Effects of thiopental on transport and metabolism of glutamate in cultured cerebellar granule neurons. Neurochem Int 37(2-3):207-215.

Sevcik C. 1980. Differences between the actions of thiopental and pentobarbital in squid giant axons. J Pharmacol Exp Ther 214(3):657-663.

Sokoloff L, Reivich M, Kennedy C, Des Rosiers MH, Patlak CS, Pettigrew KD, Sakurada O, Shinohara M. 1977. The [14C] deoxyglucose method for the measurement of local cerebral glucose utilization: theory, procedure, and normal values in the conscious and anesthetized albino rat. J Neurochem 28:897-916

Sonnay S, Duarte JMN, Just N, Gruetter R. 2016. Compartmentalised energy metabolism supporting glutamatergic neurotransmission in response to increased activity in the rat cerebral cortex: a 13C MRS study in vivo at 14.1 T. J Cereb Blood Flow Metab 36(5):928-940.

Strang RHC, Bachelard HS. 1973. Rates of cerebral glucose utilization in rats anaesthetized with phenobarbitone. J Neurochem 20:987-996.

Sugimura M, Kitayama S, Morita K, Irifune M, Takarada T, Kawahara M, Dohi T. 2001. Effects of volatile and intravenous anesthetics on the uptake of GABA, glutamate and dopamine by their transporters heterologously expressed in COS cells and in rat brain synaptosomes. Toxicol Lett 123(1):69-76.

Swanson RA, Seid LL. 1998. Barbiturates impair astrocyte glutamate uptake. Glia 24(4): 365-371.

Wang J, Jiang L, Jiang Y, Ma X, Chowdhury GM, Mason GF. 2010. Regional metabolite levels and turnover in the awake rat brain under the influence of nicotine. J Neurochem, 113(6):1447-1458.

Weiss GB, Hertz L, Goodman FR. 1972. Drug-induced alterations in respiration of rat brain cortex and striatum slices in a carbon dioxide-bicarbonate-buffered medium. Biochem Pharmacol, 21(5):625-634.

Yu AC, Hertz E, Hertz L. 1983. Effects of barbiturates on energy and intermediary metabolism in cultured astrocytes. Prog Neuropsychopharmacol Biol Psychiatry 7(4-6):691-696.